



Ice sheet influence on atmospheric circulation explains the patterns of Pleistocene alpine glacier records in North America

Joseph P. Tulenko^{a,*}, Marcus Lofverstrom^b, Jason P. Briner^a

^a Department of Geology, University at Buffalo, Buffalo, NY 14260, United States of America

^b Department of Geosciences, University of Arizona, Tucson, AZ 85721, United States of America

ARTICLE INFO

Article history:

Received 30 April 2019

Received in revised form 5 November 2019

Accepted 18 January 2020

Available online xxxx

Editor: L. Robinson

Keywords:

alpine glaciers

Laurentide Ice Sheet

Marine Isotope Stage 4

Marine Isotope Stage 2

Beringia

Western US

ABSTRACT

We explore the hypothesis that the relative size of Pleistocene ice sheets in North America modulated regional climate and alpine glaciation. We compare Pleistocene alpine glacier chronologies across North America with a comprehensive general circulation model using reconstructed ice sheet extents at peak glacial conditions during Marine Isotope Stage (MIS) 2 and MIS 4. The effect of continent-wide ice sheets on atmospheric circulation during MIS 2 led to warming in Beringia and cooling in the western US; less expansive ice sheets during MIS 4 resulted in weaker ice sheet modulation of atmospheric circulation. This led to preservation of MIS 4 moraines in Beringia due to limited MIS 2 glaciation (resulting in a MIS 2/4 moraine sequence) and overriding of MIS 4 moraines – for sites with existing chronologies – in the western United States during MIS 2 (resulting in a MIS 2/6 moraine sequence). Our results highlight how influential ice sheets are for regional climate conditions.

© 2020 Elsevier B.V. All rights reserved.

1. Introduction

Climate evolution throughout the Pleistocene was characterized by successions of cold and warm periods that resulted in multiple generations of glacier build-up and decay (Lisiecki and Raymo, 2005; Mix, 1987). These glacial – interglacial cycles were largely paced by fluctuations in global climate forcing mechanisms such as insolation and greenhouse gas concentrations (Bereiter et al., 2015; Berger and Loutre, 1991). However, the spatial expression of orbitally-paced climate cycles may be modulated by regional forcing mechanisms. In that regard, alpine glaciers are valuable proxies for regional climate variations because they respond sensitively to climate change and leave behind a rich record of their past advance culminations. To date, most alpine glacier studies focus on glacier advances during and following the Last Glacial Maximum (LGM; 26–19 ka; Clark et al., 2009) since deposits of this age remain well-preserved and chronologic constraints are more precise relative to those from earlier glaciations. Yet, studying alpine glacier patterns over multiple glacial cycles, where available, can help identify regionally-dependent, but persistent features in the climate system (e.g. Gillespie and Molnar, 1995).

Alpine glacier records spanning the middle and late Pleistocene in North America are abundant and provide an opportunity to

evaluate regional glacier response to climate forcing. However, in Beringia and the western United States (US) – where detailed records of alpine glaciation exist in North America – moraine records reveal penultimate advances (advances prior to Marine Isotope Stage 2; 29–11.7 ka; Lisiecki and Raymo, 2005) of distinctly different ages between the two locations. Furthermore, the driver of each respective pattern of glaciation remains debated. For example, a recurrent hypothesis explains the moraine pattern in Beringia by moisture availability forced by variations in the extent of the Bering Land Bridge (Brigham-Grette, 2001; Briner et al., 2005). On the other hand, in the western US, records suggest that alpine glaciers fluctuated in unison with the global pattern of ice volume (Laabs et al., 2017; Lisiecki and Raymo, 2005).

In regard to climate evolution during MIS 2, prior work has presented evidence for a possible link between regional climate variability in North America and the North American ice sheets, primarily the Laurentide Ice Sheet (LIS). For example, alpine glacier records from across the western US indicate asynchronous MIS 2 culminations, a pattern hypothesized to be related to the presence and subsequent retreat of the LIS (e.g. Licciardi et al., 2004). Additionally, the presence of extensive pluvial lakes in the now-arid Great Basin during MIS 2 has long been hypothesized as the result of a southward shift in the North Pacific storm tracks forced by the continent-wide LIS (e.g. COHMAP Members, 1988).

Modeling efforts have also implicated the LIS as an important forcing mechanism on regional climate in North America (Manabe and Broccoli, 1985; Roe and Lindzen, 2001; Otto-Bliesner et

* Corresponding author.

E-mail address: jptulenk@buffalo.edu (J.P. Tulenko).

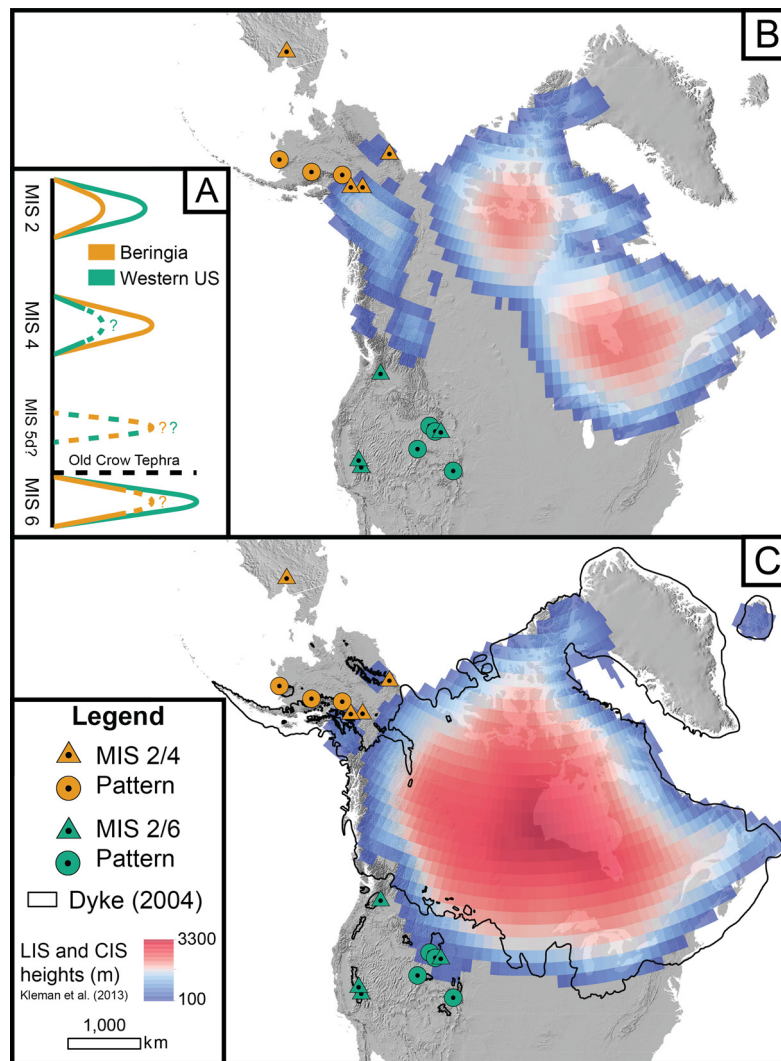


Fig. 1. A) Relative time-distance diagram for North American alpine glaciation depicting MIS 2/4 and MIS 2/6 moraine sequences for Beringia and the western US, respectively. The old crow tephra, a ubiquitous ash marker layer in eastern Beringia, serves as an important stratigraphic horizon separating MIS 4 and MIS 6 deposits at 124 ± 10 ka (Preece et al., 2011). We also include a possible but unconfirmed MIS 5d advance (due to high degree of scatter in moraine ages) for both Beringia and the western US (in dashed lines). B) Reconstructed ice sheet extents for North America during MIS 4 (Kleman et al., 2013). C) Reconstructed ice sheet extents (colored; Kleman et al., 2013) and mapped maximum ice sheet extents (black outline; Dyke, 2004) for North America during MIS 2. High-confidence alpine glacier moraine chronologies denoted by circles; low-confidence chronologies denoted by triangles. (For interpretation of the colors in the figure(s), the reader is referred to the web version of this article.)

al., 2006; Herrington and Poulsen, 2011). The most recent findings suggest that the height and lateral extent of the LIS led to limited mountain glacier expansion in Beringia during the LGM (Löfverström and Liakka, 2016), and that increasing LIS height yielded relatively warmer conditions in the Arctic (Liakka and Löfverström, 2018). It has also been found that warming upstream from the developing LIS during MIS 5d may have hindered further expansion of the ice sheet at that time (Herrington and Poulsen, 2011) While much work has been done to model the effect of the LIS on North American climate, the influence of the LIS on regional climate over multiple glacial cycles has yet to be scrutinized against local climate proxies (e.g. alpine glaciers). Here, we compile penultimate moraine chronologies in Beringia and the western US and compare them to output from a comprehensive general circulation model that was run in Löfverström et al. (2014) and to the Transient Climate Evolution of the past 21 kyr experiments (TraCE 21; Liu et al., 2009). We find that the pattern of alpine glaciation in North America is best explained by anomalous summer temperatures in both Beringia and the western US forced by fluctuations in the lateral extent of the LIS, particularly whether or not the ice

sheet complex was “continent-wide” and thus converged with the Cordilleran Ice Sheet to the west (CIS).

2. North American mountain glacier chronologies

Due to the size and persistence of the CIS and the LIS, alpine glacier moraine records are restricted exclusively to mountain ranges west of the ice sheets in Beringia, and south of the ice sheets in the western US. Through decades of detailed mapping and dating of moraines dispersed throughout both Beringia and the western US, knowledge of the timing and relative extent of the last two major glaciations in North America is substantial. In both regions, the presence of LGM and deglacial moraines (i.e. MIS 2) is ubiquitous (e.g., Briner et al., 2017; Leonard et al., 2017; Phillips, 2017; Pierce et al., 2018). However, whereas penultimate moraines deposited during the most extensive late Pleistocene glaciation in Beringia date to MIS 4 (71–57 ka) (Fig. 1A; e.g., Kaufman et al., 2011; Tulenko et al., 2018), penultimate moraines were deposited toward the end of MIS 6 (~150–130 ka; Fig. 1) in the western US, and there is no well-documented evidence of preserved MIS 4 moraines (e.g., Licciardi and Pierce, 2008; Pierce, 2003). Thus, the

current knowledge of glacial patterns in North America indicates a strictly MIS 2/4 pattern throughout Beringia and a strictly MIS 2/6 pattern throughout the western US, as all currently observed MIS 2 advances likely overrode any deposits from MIS 4 in the western United States. We note that the LGM is only a subset of MIS 2, and any further reference to MIS 2 moraines includes both LGM and deglacial moraines.

Multiple lines of evidence support the moraine patterns outlined above for Beringia and the western US, yet we cannot rule out possible exceptions. While nowhere in Beringia is there a well-documented MIS 2/6 sequence, there are locations in the western US where chronologic scatter may leave open the possibility of preserved MIS 4 moraines. The most robust chronologies available generally use cosmogenic nuclide exposure dating because few other techniques can be used to directly date moraines, particularly penultimate moraines. However, multiple studies have outlined potential pitfalls to dating moraines using cosmogenic nuclides (e.g. Putkonen and Swanson, 2003). For example, moraine degradation can skew ages from older moraines such as those deposited before MIS 2. Because degradation results in ages younger than the age of moraine deposition, it is sometimes difficult to know whether younger-than-expected ages are the result of moraine deposition during MIS 4 – or even MIS 5d (Fig. 1A; e.g. Phillips et al., 1990; Dortch et al., 2010) – or if moraines deposited during MIS 6 have been significantly degraded. In studies that date old moraines, it is most often assumed that older ages more reliably represent the timing of moraine deposition (e.g. Phillips et al., 1997; Briner et al., 2005). Regardless of moraine dating challenges, we find that seven sites (three in Beringia, four in the western US) have sufficiently well-constrained chronologies to allow high confidence in MIS 4 versus MIS 6 age assignments of penultimate moraines (circles in Fig. 1; Table S1). We make note of eight additional sites (four in Beringia and four in the western US) where a higher degree of uncertainty in the moraine chronology leads to low-confidence age assignments in support of MIS 4 or MIS 6 moraines (triangles in Fig. 1; Table S1). We define the difference between high and low-confidence age assignments on penultimate moraines in the following way: if there is a coherent cluster of ages on one moraine that all overlap within 1 standard deviation of their uncertainties, we take those to represent a high degree of certainty in age assignment for that moraine, whatever that age may be. Otherwise, if there are too few ages or ages that do not overlap within uncertainty on a single moraine, yet most ages still bin within either the MIS 4 or MIS 6 time windows, we assign only a low degree of certainty in age assignment (see Table S1; sufficient versus not sufficient statistical overlap). While we consider all currently available data, we recognize that these ideas can be tested further with additional moraine dating studies in the future.

3. Model simulations

We base our analysis on the LGM (21 ka; note that any further mention of the LGM refers to this specific time slice within MIS 2 when the LIS was largest) and MIS 4 (66 ka) global climate simulations that were run and described in Löffverström et al. (2014). These “time slice” simulations were run with the NCAR CAM3 at T85 resolution (ca. 1.4° horizontal grid spacing), coupled to a mixed-layer ocean with implied ocean heat transport derived from an equilibrated LGM simulation with the fully coupled NCAR CCSM3 (Brandefelt and Otto-Bliesner, 2009). The atmospheric greenhouse gases and orbital configuration were set to appropriate values for each time slice, while land-sea margins and vegetation were kept at their pre-industrial configuration in non-glaciated areas. Ice-sheet extents and topographies were prescribed using data-constrained reconstructions (Kleman et al., 2013). Here, we focus on comparisons between the “continent-wide glacial”

LGM simulations and what we describe as the “incomplete glacial” MIS 4 simulations, where “continent-wide” and “incomplete” refer to whether or not the LIS extended sufficiently far west to coalesce with the CIS, and thus notably disrupt atmospheric circulation (Löffverström et al., 2014; Lora et al., 2016). We also focus only on mean summer (June–July–August; JJA) surface air temperatures and annual cumulative precipitation since for alpine glaciers, annual ablation is primarily dependent on summer melt (Ohmura et al., 1992), and annual accumulation has been shown to be roughly equivalent to annual precipitation (Braithwaite, 2008). While we only present JJA surface air temperature and cumulative precipitation in this paper, all results from the simulations presented in Löffverström et al. (2014) are available online in the NOAA paleoclimate data archive (<https://www.ncdc.noaa.gov/paleo/study/26612>). To isolate the role of ice sheet forcing on North American climate, we compare the LGM and MIS 4 simulations with a sensitivity experiment for each time slice that uses identical forcings as their respective full simulations – atmospheric CO₂ concentrations set to 185 ppm for 21 ka and 195 ppm for 66 ka, and insolation set to appropriate values at 21 ka and 66 ka, respectively – but modern topography and vegetation cover (i.e. the only Northern Hemisphere ice sheet in the sensitivity simulation is the modern Greenland Ice Sheet; Table S2). Subtracting the sensitivity simulations from the full simulations gives a range of anomalies, which are a first-order indication of the climate response to the ice sheets at each time slice (Fig. 2A–D). We further analyze how climate is impacted specifically by differences in ice sheet topography between the LGM and MIS 4 simulations by subtracting the MIS 4 ice sheet sensitivity anomalies (Fig. 2B and 2D) from the LGM ice sheet sensitivity anomalies (Fig. 2A and 2C; those results are found in Fig. 2E and 2G). Finally, we subtract the full MIS 4 simulation from the full LGM simulation (Fig. 2F and 2H) for comparison between what we refer to as the “ice sheet effect” (Fig. 2E and 2G) and the differences between the full simulations.

We further explore the ice sheet influence on North American climate using model output from the fully coupled TraCE 21 simulation (Liu et al., 2009), spanning 21 ka to present. TraCE 21 ka uses the same atmosphere model (NCAR CAM3) as the “time slice” simulations, but is a fully coupled simulation that uses the ICE-5G topographies from Peltier (2004). Although TraCE 21 only covers our MIS 2 time period of interest, we find that the ice margin is qualitatively similar to the MIS 4 reconstruction in Kleman et al. (2013) at 13 ka; we thus use this point in time in the “transient” simulation as a process analogue for our “incomplete” ice sheet configuration (panel C in Fig. S2). While we recognize that boundary conditions such as insolation and greenhouse gas concentrations at ~13 ka and 66 ka are significantly different and would produce incomparable full climatologies, we focus exclusively on how North American climate responds to the transition from “full” to “incomplete” North American ice sheet configurations within the TraCE 21 ka experiment. To compare climatologies specifically in Beringia and the western US, we isolate grid cells that cover each respective location (Fig. S3) and extract time-series of annual, mean summer (JJA) and mean winter (December–January–February; DJF) surface temperature and precipitation anomalies with respect to a 200-year pre-industrial climatology from the end of the simulation (Figs. 3, S4 and S5). In addition, we extract time-series of surface temperature and precipitation anomalies for all single-forcing experiments from TraCE 21, where each forcing mechanism is allowed to evolve through time while all other forcing mechanisms remain constant (Liu et al., 2009; He, 2011). While we only focus on the ice-sheet single-forcing experiment from TraCE 21, we present time-series for all other single forcing experiments in the supplement (i.e. meltwater, insolation and greenhouse gases; Figs. S4 and S5).

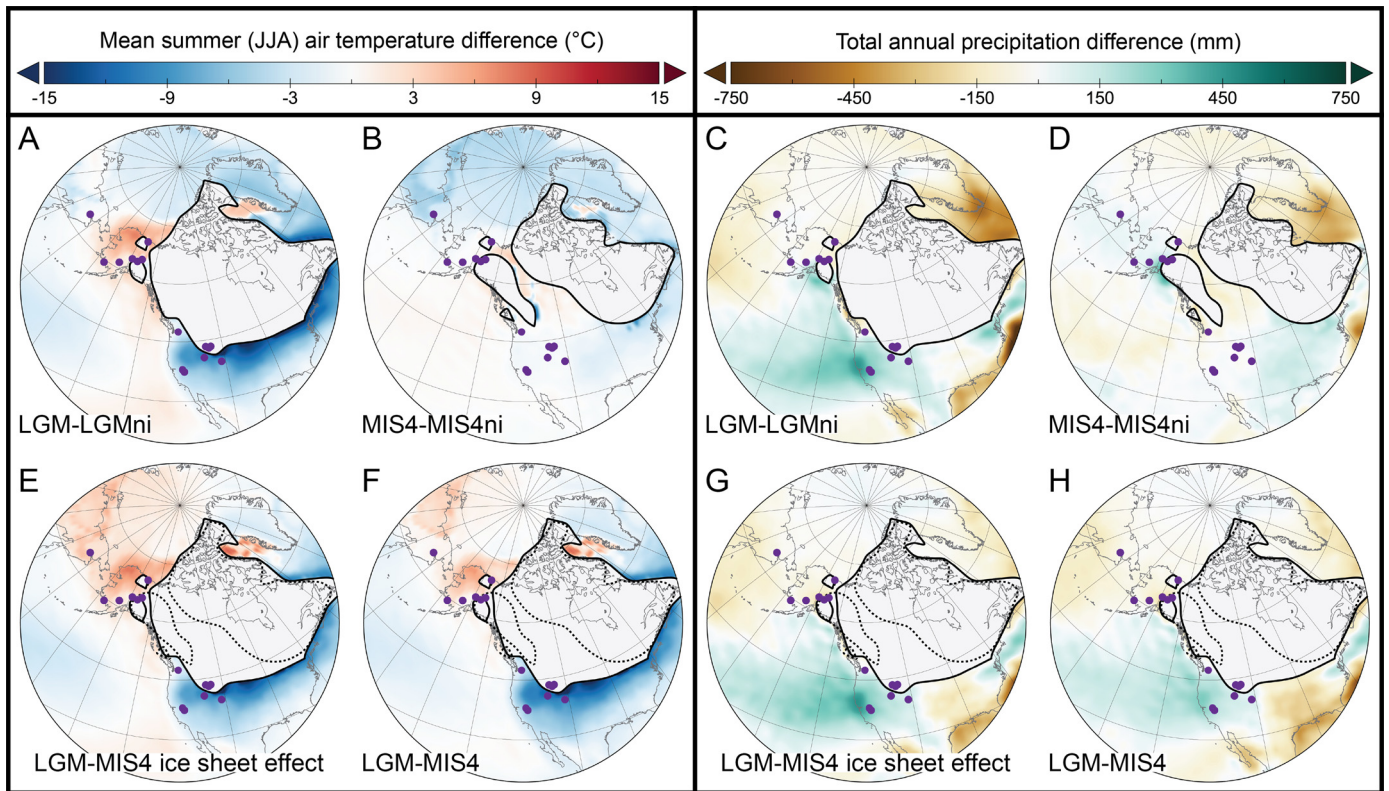


Fig. 2. North America climatologies during MIS 2 and 4. A) and C) show JJA temperature and annual cumulative precipitation differences, respectively, for the 21 ka (LGM) simulation with a continent-wide LIS configuration minus the 21 ka sensitivity simulation with no ice sheets (i.e. the same simulation only using modern topography and vegetation cover; LGMni). B) and D) show corresponding difference fields for the 66 ka (MIS 4) simulation with the incomplete LIS configuration minus the 66 ka sensitivity simulation with no ice sheets (i.e. the same simulation only using modern topography and vegetation cover; MIS4ni). E) and G) show computed differences between A)–B) and C)–D), respectively, and demonstrate climate in North America was more strongly modulated by ice sheet forcing during the LGM compared to MIS 4. Finally, F) and H) show the computed difference between the full 21 ka (LGM) and 66 ka (MIS 4) simulations. Ice sheet outlines for the LGM and MIS 4 from Kleman et al. (2013), and colored dots represent locations of alpine glacier chronologies (see Table S1). Note that we mask out values of grid cells covered by the ice sheets for display purposes.

4. Results

The time slice simulations indicate that with a continent-wide LIS configuration (during the LGM), surface air temperature in Beringia (particularly in Alaska, where a majority of Beringian moraine chronologies are located) is relatively warm compared to the sensitivity simulation with modern topography (no LIS) and vegetation (Fig. 2A). Conversely, the surface temperature in Beringia is much less impacted by the incomplete LIS configuration (during MIS 4) (Fig. 2B). Furthermore, an inverse climate pattern occurs for the western US, where the surface temperature is relatively colder with the presence a continent-wide LIS configuration (LGM) compared to the incomplete LIS configuration (MIS 4) (Figs. 2A and 2B). The difference between LGM and MIS 4 surface temperature sensitivity to ice sheet forcing highlights a greater warming in Beringia and cooling in the western US with the continent-wide LIS configuration compared to the incomplete LIS configuration (Fig. 2E). We also observe greater ice-sheet-induced warming throughout the Arctic with a continent-wide LIS configuration versus the incomplete LIS configuration (Fig. 2E; Liakka and Löfverström, 2018). As a final result, the difference in surface temperature between each full time slice simulation shows a relatively warmer climate in Beringia and colder climate in the western US during the LGM compared to MIS 4 (Fig. 2F). It is important to note that in both time slices, simulated temperatures in our study area are colder than present (see Fig. S1). In addition, we observe the same pattern for total annual precipitation; Beringia is relatively dry and the western US is relatively wet during the LGM compared to MIS 4 (Fig. 3H). Similar to surface temperature, this

trend is also mainly driven by differences in LIS configurations between the LGM and MIS 4 (Fig. 3G).

The results from the transient (TraCE 21) ice sheets single forcing exercise reveal that summer temperatures in both Beringia (Fig. 3B) and the western US (Fig. 3F) were strongly modulated by the presence of continent-wide LGM (21 ka) ice sheets. We identify a threshold extent of the LIS at ~ 13 ka (when the CIS and LIS were no longer coalesced) at which point the ice sheet influence on atmospheric circulation became less influential on the climate in Beringia and the western US. Thus, ~ 13 ka is when ice sheet size transitioned to the incomplete extent, similar to the ice sheet configuration during MIS 4. Results from the transient simulation suggest that the evolution from continent-wide to incomplete glacial configurations, and attendant climate transition, validates the use of 13 ka as a process analogue for the MIS 4 climatology in our time slice simulations (Fig. 2).

Both the “time slice” and “transient” (TraCE 21) modeling results indicate a stark contrast between ice sheet influence on climate during the LGM (21 ka) compared with MIS 4 (or 13 ka in the transient simulation). The continent-wide LGM (21 ka) ice sheet configuration induces a permanent anticyclone (not shown) over much of northern North America due to strong diabatic surface cooling and mechanical wave forcing from the westerlies impinging on the ice-sheet topography (Löfverström and Liakka, 2016). The impact of LIS topography thus re-organizes the stationary waves over the North Pacific (see Löfverström et al., 2014, Fig. 2, 4, and 6; Lora et al., 2016, Fig. 4) and induces increased meridional heat transport into Beringia, as shown previously (e.g. Manabe and Broccoli, 1985; Otto-Bliesner et al., 2006; Roe and Lindzen, 2001). Additionally, and perhaps more importantly for

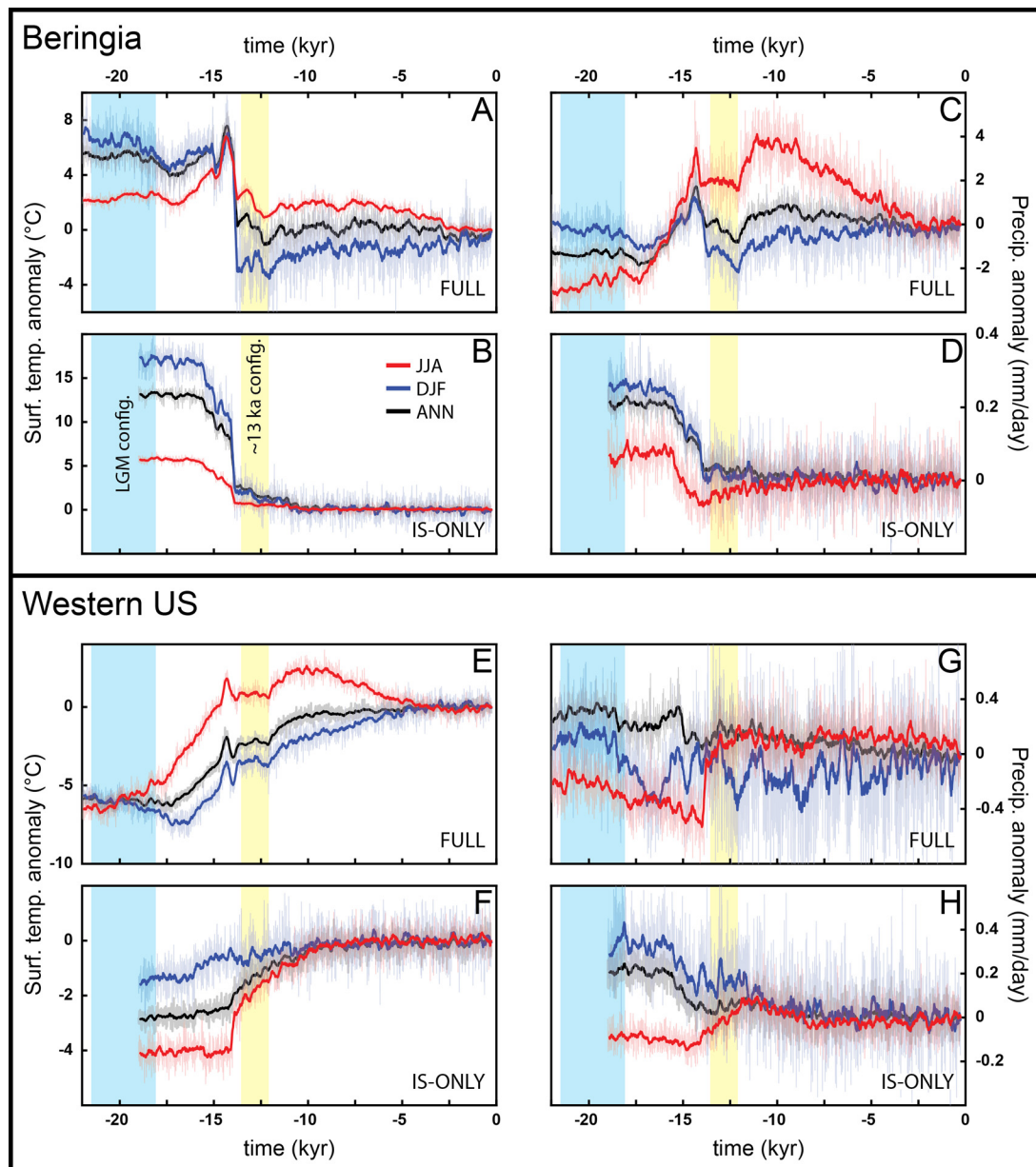


Fig. 3. Time series of temperature and precipitation anomalies for Beringia (panels A – D) and the western US (panels E–H) from TraCE 21 simulations. Both regions (Beringia and the western US) are indicated in Fig. S3. All panels on the left side are temperature anomalies and all panels on the right side are precipitation anomalies. Panels A, C, E, and G are time series from the full TraCE 21 simulation, and panels B, D, F, and H are time series from the single forcing ice sheet simulation. Solid lines indicate a 100-year running mean for each time series. Annual temperature and precipitation anomalies are in black, mean summer (June–July–August) anomalies are in red, and mean winter (December–January–February) anomalies are in blue (see inset legend in panel B). The time intervals within the transient TraCE 21 simulation when the ice sheet configurations from Peltier (2004) most closely resemble the ice sheet configurations from the “time slice” simulations at the culmination of the LGM (LGM = blue; ~13 ka = yellow).

summer air temperature anomalies, continent-wide ice sheet conditions paired with lower sea surface temperatures during the LGM act to reduce cloudiness over Beringia and enhance short-wave radiation that reaches the land surface (Löfverström and Liakka, 2016). On the other hand, summer air temperatures were reduced in the western US as a result of the anticyclone over the continent-wide LGM (21 ka) ice sheet configuration.

We find that the total annual precipitation delivered to the western US increased in response to a continent-wide ice sheet configuration, particularly in the winter season when meridional temperature gradients are strengthened and the mid-latitude stormtracks are most active (e.g. Shaw et al., 2016). In contrast, during the incomplete glacial MIS 4 (and at 13 ka), the westerly mean flow was deflected around the LIS by the pre-existing sta-

tionary wave response to the Cordillera uplands, and therefore the incomplete ice sheet configuration did not significantly alter the stationary wave over the North Pacific (Löfverström et al., 2014). By reducing the impact of the LIS on North Pacific atmospheric circulation during MIS 4 (and at 13 ka), climate in Beringia remained relatively cold and wet while climate in the western US remained relatively warm and dry compared to the LGM.

In regard to precipitation over both Beringia and the western US, we find discrepancies between the “time slice” simulations and the process analogue “transient” (TraCE 21) simulations. In particular, all results from the ice sheets sensitivity simulation (Fig. 3D) and winter precipitation in the full simulation (Fig. 3C) in TraCE 21 show a notable transition from higher precipitation anomalies at 21 ka to lower precipitation anomalies around and following

13 ka in Beringia. This is in direct contrast to results from the “time slice” simulations run in Löffverström et al. (2014) that show a relatively dry annual climate in Beringia during the LGM (21 ka) compared to MIS 4, driven largely by ice sheet forcing. It is possible that TraCE 21 shows wetter 21 ka (LGM) climate, particularly in the winter, simply because air temperatures were warmer relative to 13 ka (MIS 4), and that the model does not capture the general reduction in cloudiness and moisture delivery to Beringia at 21 ka as observed by Löffverström et al. (2014). TraCE 21 was also run at a lower spatial resolution (T31, or around 3.8° grid spacing compared to T85, or around 1.4° grid spacing in Löffverström et al., 2014), which potentially can account for some of these discrepancies (e.g. Löffverström and Liakka, 2018). Regardless, we suggest that glaciers in both Beringia and the western US were likely more sensitive to changes in summer air temperatures than cumulative precipitation (e.g. Rupper and Roe, 2008).

5. Discussion

The results from the “time slice” and “transient” simulations help explain the observed alpine glacial moraine sequences across North America. The climatic conditions across North America resulting from a continent-wide ice sheet configuration favor relatively less extensive glaciers in Beringia and relatively more extensive glaciers in the western US during MIS 2. However, an incomplete ice sheet configuration during MIS 4 produced climatic conditions that would have led to relatively more extensive glaciers in Beringia, and relatively less extensive glaciers in the western US. Thus, both the “time slice” and “transient” simulations support the observed record of moraines dating to MIS 4 directly outboard of MIS 2 moraines in Beringia, and moraines dating to MIS 6 directly outboard of MIS 2 moraines in the western US.

Generally, paleoclimate records from North America that span from the middle Pleistocene through the late Pleistocene are rare. In Beringia, a Si/Ti record – interpreted as a proxy for summer productivity – from sediments deposited in Lake El'Gygytyn in eastern Siberia suggests that summer conditions during MIS 4 were the coldest on record (Melles et al., 2012), and colder than both MIS 2 and 6. Similarly, a compilation of loess records from interior Alaska implies more extreme glacial conditions in the region during MIS 4 compared to MIS 2 (Jensen et al., 2016). In contrast, a number of composite speleothem records from the western US interpreted as proxies for mean annual temperature (assuming variations in precipitation $\delta^{18}\text{O}$ can be accounted for) indicate a more pronounced temperature depression during MIS 2 compared to MIS 4 (Lachniet et al., 2014; Moseley et al., 2016). A compilation of hydroclimate records from the western US supports the likelihood that a continent-wide LIS configuration forced an equatorward hydroclimate shift in western North America during the LGM (e.g., Oster et al., 2015). This resulted in increased precipitation delivery primarily to the southwestern US. Thus, the available paleoclimate records support the interpretation that varying LIS configurations led to the observed differences in climate, and hence the Pleistocene moraine records in Beringia and the western US.

Our analysis may indicate that, far outside of North America where the LIS influence is less strong, penultimate moraines may not follow the regional climate anomalies that we have outlined in North America. For example, data from the Southern Alps in New Zealand, where alpine glaciers were likely free from any influence of North American ice sheets (e.g. Otto-Bliesner et al., 2006), reveal both MIS 2/4 (Schaefer et al., 2015) and MIS 2/6 (Putnam et al., 2013) moraine sequences in adjacent valleys. While additional absolute chronologies for penultimate moraines do not yet exist in New Zealand, detailed mapping and relative dating of glacial deposits suggest that both MIS 2/4 and MIS 2/6 sequences are present throughout the Southern Alps (Barrell, 2011). Further-

more, records from southern Patagonia indicate a similar pattern in penultimate moraine ages, where MIS 2/4 (Peltier et al., 2016), MIS 2/6 (Kaplan et al., 2005) and even MIS 2/8 (Hein et al., 2009) moraine sequences are observed. Returning to the Northern Hemisphere, Lifton et al. (2014) synthesize findings for possible MIS 2/4, MIS 2/6 and even MIS 2/5d moraine sequences in the Tien Shan, central Asia. In addition, moraine sequences in the northern mountains of the Iberian Peninsula may include both MIS 4 and MIS 6 moraines (Rodríguez-Rodríguez et al., 2016). The presence of MIS 2/4 and MIS 2/6 moraine sequences in neighboring valleys around the world indicates that full glacial conditions were achieved during both MIS 2 and MIS 4 somewhat equally. This is unlike North America, where full glacial conditions were achieved during MIS 4 exclusively in Beringia and during MIS 2 exclusively in the western US, owing to the strong modulating effects related to LIS size.

6. Conclusions

We demonstrate that climatic output from two comprehensive global climate models (Löffverström et al., 2014; Liu et al., 2009) can qualitatively explain the anomalous alpine glacier moraine patterns preserved in North America. Results from model sensitivity testing indicate that climate in both Beringia and the western US was significantly influenced by the continent-wide ice sheet configuration during MIS 2, which warmed Beringia and cooled the western US. We conclude that during the MIS 2, re-organization of atmospheric circulation forced by more extensive ice sheets led to limited glacier advances and the widespread preservation of MIS 4 moraines throughout Beringia, and anomalously extensive glacier advances thus far observed in the western US leading to the overriding of MIS 4 moraines. We expand on the previous hypothesis put forth by Gillespie and Molnar (1995) by confirming that a regional climate mechanism drove the preservation of MIS 4 moraines in some locations (Beringia in this case), but at the same time, that regional climate mechanism likely hindered MIS 4 advances in the western US.

In a global context, the pattern of alpine glaciation in North America demonstrates how local forcing mechanisms such as large North American ice sheets are important modulators of regional climate. While there are known difficulties associated with accurately reconstructing pre-LGM ice sheets (Batchelor et al., 2019), we assume that any discrepancies do not affect our qualitative findings. Especially given that the “time-slice” and “transient” simulations use independent ice sheet reconstructions from Kleman et al. (2013) and Peltier (2004), respectively, yet still produce similar qualitative results. However, our results are qualitative and highlight the need for (1) additional, precise alpine glacier chronologies worldwide, and (2) improvements to observation-based reconstructions of ice sheet configurations, particularly prior to the LGM (e.g. Batchelor et al., 2019), that are incorporated in global climate models (e.g., Kageyama et al., 2017).

Declaration of competing interest

The authors declare that they have no known competing financial interests or personal relationships that could have appeared to influence the work reported in this paper.

Appendix A. Supplementary material

Supplementary material related to this article can be found online at <https://doi.org/10.1016/j.epsl.2020.116115>.

References

- Barrell, D., 2011. Quaternary Glaciers of New Zealand. *Developments in Quaternary Sciences*, vol. 15. Elsevier, pp. 1047–1064.

- Batchelor, C.L., Margold, M., Krapp, M., Murton, D.K., Dalton, A.S., Gibbard, P.L., et al., 2019. The configuration of Northern Hemisphere ice sheets through the quaternary. *Nat. Commun.* 10 (1), 3713. <https://doi.org/10.1038/s41467-019-11601-2>.
- Bereiter, B., Eggleston, S., Schmitt, J., Nehrbass-Ahles, C., Stocker, T.F., Fischer, H., et al., 2015. Revision of the EPICA Dome C CO₂ record from 800 to 600 kyr before present. *Geophys. Res. Lett.* 42 (2), 542–549. <https://doi.org/10.1002/2014GL061957>.
- Berger, A., Loutre, M.-F., 1991. Insolation values for the climate of the last 10 million years. *Quat. Sci. Rev.* 10 (4), 297–317.
- Braithwaite, R.J., 2008. Temperature and precipitation climate at the equilibrium-line altitude of glaciers expressed by the degree-day factor for melting snow. *J. Glaciol.* 54 (186), 437–444.
- Brandefelt, J., Otto-Bliesner, B., 2009. Equilibration and variability in a last glacial maximum climate simulation with CCSM3. *Geophys. Res. Lett.* 36 (19).
- Brigham-Grette, J., 2001. New perspectives on Beringian Quaternary paleogeography, stratigraphy, and glacial history. *Quat. Sci. Rev.* 20 (1), 15–24. [https://doi.org/10.1016/S0277-3791\(00\)00134-7](https://doi.org/10.1016/S0277-3791(00)00134-7).
- Briner, J.P., Kaufman, D.S., Manley, W.F., Finkel, R.C., Caffee, M.W., 2005. Cosmogenic exposure dating of late Pleistocene moraine stabilization in Alaska. *Geol. Soc. Am. Bull.* 117 (7–8), 1108–1120.
- Briner, J.P., Tulenko, J., Young, N., Baichtal, J., Lesnek, A., 2017. The last deglaciation of Alaska. *Cuad. Investig. Geogr.* 43 (2), 429–448.
- Clark, P.U., Dyke, A.S., Shakun, J.D., Carlson, A.E., Clark, J., Wohlfarth, B., et al., 2009. The last glacial maximum. *Science* 325 (5941), 710–714. <https://doi.org/10.1126/science.1172873>.
- COHMAP Members, 1988. Climatic changes of the last 18,000 years: observations and model simulations. *Science*, 1043–1052.
- Dortch, J.M., Owen, L.A., Caffee, M.W., Li, D., Lowell, T.V., 2010. Beryllium-10 surface exposure dating of glacial successions in the Central Alaska Range. *J. Quat. Sci.* 25 (8), 1259–1269.
- Dyke, A.S., 2004. An outline of North American deglaciation with emphasis on central and northern Canada. *Develop. Quatern. Sci.* 2, 373–424.
- Gillespie, A., Molnar, P., 1995. Asynchronous maximum advances of mountain and continental glaciers. *Rev. Geophys.* 33 (3), 311–364.
- He, F., 2011. Simulating transient climate evolution of the last deglaciation with CCSM3. PhD thesis. Dep. of Atmos. and Oceanic Sci., Univ. of Wisconsin-Madison. 161 pp.
- Hein, A.S., Hulton, N.R., Dunai, T.J., Schnabel, C., Kaplan, M.R., Naylor, M., Xu, S., 2009. Middle Pleistocene glaciation in Patagonia dated by cosmogenic-nuclide measurements on outwash gravels. *Earth Planet. Sci. Lett.* 286 (1–2), 184–197.
- Herrington, A.R., Poulsen, C.J., 2011. Terminating the last interglacial: the role of ice sheet–climate feedbacks in a GCM asynchronously coupled to an ice sheet model. *J. Climate* 25 (6), 1871–1882.
- Jensen, B.J.L., Evans, M.E., Froese, D.G., Kravchinsky, V.A., 2016. 150,000 years of loess accumulation in central Alaska. *Quat. Sci. Rev.* 135, 1–23. <https://doi.org/10.1016/j.quascirev.2016.01.001>.
- Kageyama, M., Albani, S., Braconnot, P., Harrison, S.P., Hopcroft, P.O., Ivanovic, R.F., et al., 2017. The PMIP4 contribution to CMIP6–Part 4: Scientific objectives and experimental design of the PMIP4–CMIP6 last glacial maximum experiments and PMIP4 sensitivity experiments. *Geosci. Model Dev.* 10 (11), 4035–4055.
- Kaplan, M.R., Douglass, D.C., Singer, B.S., Ackert, R.P., Caffee, M.W., 2005. Cosmogenic nuclide chronology of pre-last glacial maximum moraines at Lago Buenos Aires, 46 S, Argentina. *Quat. Res.* 63 (3), 301–315.
- Kaufman, D.S., Young, N.E., Briner, J.P., Manley, W.F., 2011. Alaska paleo-glacier atlas (version 2). In: Ehlers, J., Gibbard, P.L., Hughes, P. (Eds.), *Quaternary Glaciations – Extent and Chronology*. In: *Developments in Quaternary Science*, vol. 15. Amsterdam, Netherlands.
- Kleman, J., Fastook, J., Ebert, K., Nilsson, J., Caballero, R., 2013. Pre-LGM Northern Hemisphere ice sheet topography. *Clim. Past* 9 (5), 2365.
- Laabs, B.J.C., Licciardi, J.M., Marchetti, D.W., Munroe, J.S., Leonard, E.M., 2017. Cosmogenic nuclide exposure age limits on the penultimate glaciation in the conterminous western U.S. Paper presented at the Geological Society of America Annual Meeting, Seattle, Washington, USA.
- Lachniet, M.S., Denniston, R.F., Asmerom, Y., Polyak, V.J., 2014. Orbital control of western North America atmospheric circulation and climate over two glacial cycles. *Nat. Commun.* 5, 3805.
- Leonard, E.M., Laabs, B., Schweinsberg, A., Russell, C.M., Briner, J.P., Young, N., 2017. Deglaciation of the Colorado Rocky mountains following the last glacial maximum. *Cuad. Investig. Geogr.* 43 (2), 497–526.
- Liakka, J., Löffverström, M., 2018. Arctic warming induced by the Laurentide Ice Sheet topography. *Clim. Past* 14 (6), 887–900.
- Licciardi, J.M., Clark, P.U., Brook, E.J., Elmore, D., Sharma, P., 2004. Variable responses of western US glaciers during the last deglaciation. *Geology* 32 (1), 81–84.
- Licciardi, J.M., Pierce, K.L., 2008. Cosmogenic exposure-age chronologies of Pinedale and Bull Lake glaciations in greater Yellowstone and the Teton Range, USA. *Quat. Sci. Rev.* 27 (7–8), 814–831.
- Lifton, N., Beel, C., Hättestrand, C., Kassab, C., Rogozhina, I., Heermance, R., et al., 2014. Constraints on the late quaternary glacial history of the Inylchek and Sary-Dzaz valleys from in situ cosmogenic ¹⁰Be and ²⁶Al, eastern Kyrgyz Tian Shan. *Quat. Sci. Rev.* 101, 77–90. <https://doi.org/10.1016/j.quascirev.2014.06.032>.
- Lisiecki, L.E., Raymo, M.E., 2005. A Pliocene-Pleistocene stack of 57 globally distributed benthic δ¹⁸O records. *Paleoceanography* 20 (1). <https://doi.org/10.1029/2004PA001071>, n/a–n/a.
- Liu, Z., Otto-Bliesner, B., He, F., Brady, E., Tomas, R., Clark, P., Brook, E., 2009. Transient simulation of last deglaciation with a new mechanism for Bølling-Allerød warming. *Science* 325 (5938), 310–314.
- Löffverström, M., Caballero, R., Nilsson, J., Kleman, J., 2014. Evolution of the large-scale atmospheric circulation in response to changing ice sheets over the last glacial cycle. *Clim. Past* 10 (4), 1453–1471.
- Löffverström, M., Liakka, J., 2018. The influence of atmospheric grid resolution in a climate model-forced ice sheet simulation. *Cryosphere* 12 (4).
- Löffverström, M., Liakka, J., 2016. On the limited ice intrusion in Alaska at the LGM. *Geophys. Res. Lett.* 43 (20).
- Lora, J.M., Mitchell, J.L., Tripati, A.E., 2016. Abrupt reorganization of North Pacific and western North American climate during the last deglaciation. *Geophys. Res. Lett.* 43 (22), 11,796–11,804.
- Manabe, S., Broccoli, A., 1985. The influence of continental ice sheets on the climate of an ice age. *J. Geophys. Res., Atmos.* 90 (D1), 2167–2190.
- Melles, M., Brigham-Grette, J., Minyuk, P.S., Nowaczyk, N.R., Wennrich, V., DeConto, R.M., et al., 2012. 2.8 million years of Arctic climate change from Lake El'gygytyn, NE Russia. *Science* 337 (6092), 315–320.
- Mix, A., 1987. The oxygen-isotope record of glaciation. *Geol. N. Am.* 3, 111–135.
- Moseley, G.E., Edwards, R.L., Wendt, K.A., Cheng, H., Dublyansky, Y., Lu, Y., et al., 2016. Reconciliation of the Devils Hole climate record with orbital forcing. *Science* 351 (6269), 165–168.
- Ohmura, A., Kasser, P., Funk, M., 1992. Climate at the equilibrium line of glaciers. *J. Glaciol.* 38 (130), 397–411. <https://doi.org/10.3189/S002214300002276>.
- Oster, J.L., Ibarra, D.E., Winnick, M.J., Maher, K., 2015. Steering of westerly storms over western North America at the last glacial maximum. *Nat. Geosci.* 8 (3), 201.
- Otto-Bliesner, B.L., Brady, E.C., Clauzet, G., Tomas, R., Levis, S., Kothavala, Z., 2006. Last glacial maximum and Holocene climate in CCSM3. *J. Climate* 19 (11), 2526–2544.
- Peltier, C., Kaplan, M., Schaefer, J., Soteris, R., Sagredo, E., Aravena, J., 2016. A glacial chronology of the Strait of Magellan. Paper presented at the AGU Fall Meeting (Abstracts).
- Peltier, W., 2004. Global glacial isostasy and the surface of the ice-age Earth: the ICE-5G (VM2) model and GRACE. *Annu. Rev. Earth Planet. Sci.* 32, 111–149.
- Phillips, F., 2017. Glacial chronology of the Sierra Nevada, California, from the last glacial maximum to the Holocene. *Cuad. Investig. Geogr.* 43 (2), 527–552.
- Phillips, F.M., Zreda, M.G., Gosse, J.C., Klein, J., Evenson, E.B., Hall, R.D., et al., 1997. Cosmogenic ³⁶Cl and ¹⁰Be ages of quaternary glacial and fluvial deposits of the Wind River Range, Wyoming. *Geol. Soc. Am. Bull.* 109 (11), 1453–1463.
- Phillips, F.M., Zreda, M.G., Smith, S.S., Elmore, D., Kubik, P.W., Sharma, P., 1990. Cosmogenic chlorine-36 chronology for glacial deposits at Bloody Canyon, eastern Sierra Nevada. *Science* 248 (4962), 1529–1532.
- Pierce, K.L., 2003. Pleistocene glaciations of the Rocky Mountains. *Develop. Quatern. Sci.* 1, 63–76.
- Pierce, K.L., Licciardi, J.M., Good, J.M., Jaworowski, C., 2018. Pleistocene glaciation of the Jackson Hole area, Wyoming (2330–7102).
- Preece, S.J., Pearce, N.J.G., Westgate, J.A., Froese, D.G., Jensen, B.J.L., Perkins, W.T., 2011. Old Crow tephra across eastern Beringia: a single cataclysmic eruption at the close of Marine Isotope Stage 6. *Quat. Sci. Rev.* 30 (17), 2069–2090. <https://doi.org/10.1016/j.quascirev.2010.04.020>.
- Putkonen, J., Swanson, T., 2003. Accuracy of cosmogenic ages for moraines. *Quat. Res.* 59 (2), 255–261.
- Putnam, A.E., Schaefer, J.M., Denton, G.H., Barrell, D.J., Birkel, S.D., Andersen, B.G., et al., 2013. The last glacial maximum at 44°S documented by a ¹⁰Be moraine chronology at Lake Ohau, Southern Alps of New Zealand. *Quat. Sci. Rev.* 62, 114–141.
- Rodríguez-Rodríguez, L., Jiménez-Sánchez, M., Domínguez-Cuesta, M.J., Rinterknecht, V., Pallàs, R., Bourlès, D., 2016. Chronology of glaciations in the Cantabrian Mountains (NW Iberia) during the Last Glacial Cycle based on in situ-produced ¹⁰Be. *Quat. Sci. Rev.* 138, 31–48. <https://doi.org/10.1016/j.quascirev.2016.02.027>.
- Roe, G.H., Lindzen, R.S., 2001. The mutual interaction between continental-scale ice sheets and atmospheric stationary waves. *J. Climate* 14 (7), 1450–1465.
- Rupper, S., Roe, G., 2008. Glacier changes and regional climate: a mass and energy balance approach. *J. Climate* 21 (20), 5384–5401.
- Schaefer, J.M., Putnam, A.E., Denton, G.H., Kaplan, M.R., Birkel, S., Doughty, A.M., et al., 2015. The southern glacial maximum 65,000 years ago and its unfinished termination. *Quat. Sci. Rev.* 114, 52–60. <https://doi.org/10.1016/j.quascirev.2015.02.009>.
- Shaw, T.A., Baldwin, M., Barnes, E.A., Caballero, R., Garfinkel, C.I., Hwang, Y.T., et al., 2016. Storm track processes and the opposing influences of climate change. *Nat. Geosci.* 9, 656. <https://doi.org/10.1038/ngeo2783>.
- Tulenko, J.P., Briner, J.P., Young, N.E., Schaefer, J.M., 2018. Beryllium-10 chronology of early and late Wisconsinan moraines in the Revelation Mountains, Alaska: insights into the forcing of Wisconsinan glaciation in Beringia. *Quat. Sci. Rev.* 197, 129–141.